Bacterial Circadian Clock and Rhythms Book (eds. Ditty JL, Mackey SR, Johnson CH)
"Oscillator Structure" chapter, version 2008-07-13

Structural aspects of the cyanobacterial KaiABC circadian clock

Martin Egli[1,*] and Phoebe L. Stewart[2]

[1]Department of Biochemistry and [2]Department of Molecular Physiology and Biophysics, School of Medicine, Vanderbilt University, Nashville, TN 37232

* Corresponding author. Phone +1 (615) 343-8070. Fax: +1 (615) 322-7122. e-mail: martin.egli@vanderbilt.edu.

Abstract

The KaiABC circadian clock in the cyanobacterium *Synechococcus elongatus* can be reconstituted in vitro from three proteins in the presence of ATP. The in vitro oscillator displays the pertinent features of circadian rhythms including a self-sustained 24-hour period and temperature compensation. At every phase of the cycle there is a mixture of types of Kai complexes and the proportions of the various types are oscillating. The KaiC protein is an auto-kinase and auto-phosphatase whose phosphorylation levels oscillate over the daily period whereby KaiA and KaiB interact with KaiC to increase and decrease its phosphorylation, respectively. This chapter summarizes progress in the three-dimensional (3D) structural characterization of Kai proteins made in the last years and insights into the KaiA-KaiC interaction gained by NMR and 3D electron microscopy (EM). Despite impressive advances in the structural realm, many open questions remain regarding the control of KaiC phosphorylation by KaiA and KaiB and conformational changes accompanying the transition between the hypo- and hyper-phosphorylated states of KaiC.

1. Introduction

Recent research has shown that the cyanobacterial circadian clock is able to function without de novo synthesis of clock gene mRNAs and the proteins encoded by them, and accurate determination of the period is achieved without transcriptional/translational feedback (Tomita et al. 2005). In the model organism *Synechococcus elongatus* (*S. elongatus*) there exists a minimal timing loop *in vivo* that functions without transcription and translation and exhibits temperature compensation. Even more remarkably, it was found that the circadian clock in *S. elongatus* can be fully reconstituted in vitro by the three proteins KaiA, KaiB and KaiC in the presence of ATP (Nakajima et al. 2005). These discoveries render the KaiABC timekeeper a unique target for biochemical and biophysical analyses. Three-dimensional structures of full-length versions of the KaiA, KaiB and KaiC proteins from different cyanobacterial strains became available in 2004 (reviewed in (Johnson and Egli 2004; Golden 2004; Egli et al. 2007)) (**Figure 1**).

The first structure to be determined was that of the N-terminal pseudo-receiver domain of KaiA from *S. elongatus* (Williams et al. 2002) (**Table 1**). Afterward, the structure of the KaiC protein was initially characterized by negative-stain EM studies that revealed a homo-hexameric particle with a central opening (Mori et al. 2003; Hayashi et al. 2003). Subsequently, a crystal structure of full-length KaiA from *S. elongatus* exposed a domain-swapped dimer with three different dimer interfaces (Ye et al. 2004). One of these connects the N-terminal receiver domain with the C-terminal KaiC-interacting domain (**Figure 1A**). Further KaiA structures include those of the C-terminal dimerization and KaiC-interacting domain of KaiA from *Thermosynechococcus elongatus BP-1* (*T. elongatus*), determined separately by X-ray crystallography (Uzumaki et al. 2004) and NMR (Vakonakis et al. 2004a), and the crystal structure of the C-terminal domain of KaiA from the cyanobacterium *Anabaena* PPC7120 (Garces et al. 2004) (**Table 1**).

The crystal structure of full-length *Anabaena* KaiB revealed a thioredoxin-like fold (Garces et al. 2004) (**Figure 1B**, **Table 2**). In this structure KaiB was found to be a dimer with a loop region in the monomer contributing the majority of the interactions between the two subunits. In the crystal structures of KaiB from *Synechocystis PCC6803* (Hitomi et al. 2005) and *T. elongatus* (Iwase et al. 2005) the protein forms a tetramer with

a positively charged perimeter, a negatively charged center and a zipper of aromatic rings important for oligomerization. There is evidence based on mutational data that supports the importance of the tetrameric state of KaiB (Hitomi et al. 2005) and the C-terminal acidic region (Iwase et al. 2005) for proper clock function.

The crystal structure of the full-length KaiC protein from *S. elongatus* was determined in one of our laboratories (Pattanayek et al. 2004). As expected based on the earlier EM results the central and largest protein from the cyanobacterial clock exists in the form of a homo-hexamer with a central pore. Its shape resembles a double-doughnut whereby the N-terminal CI and the C-terminal CII halves constitute the lower and the upper rings, respectively (**Figure 1C**, **Table 3**). Twelve ATP molecules are bound between the interfaces of CI and CII domains of monomers. The key phosphorylation sites S431 and T432 were independently identified based on the crystal structure (Xu et al. 2004) and from a mass spectrometric approach (Nishiwaki et al. 2004) and map exclusively to the CII half of the protein. In the crystal structure, all six T432 sites were phosphorylated whereas four of the S431 sites were phosphorylated. The phosphorylation occurs across subunits and when S431 is phosphorylated, the hydroxyl group of T426 forms a hydrogen bond to that phosphate group (Xu et al. 2004). We took this as evidence that T426 represents a third possible phosphorylation site. These three residues (T426, S431 and T432) when mutated to alanine individually, abolish rhythmicity and the triple mutant (T426/S431/T432→A) is no longer phosphorylatable.

An NMR structure of the complex of a KaiC peptide with the C-terminal domain of KaiA showed that the C-terminal peptide of KaiC interacts with KaiA (Vakonakis and LiWang 2004) (**Table 4**). However there were suggestions from yeast two-hybrid studies that KaiA might also bind to the linker region of KaiC between the CI and CII domains (Taniguchi et al. 2001). A three-dimensional electron microscopy (EM) study of the KaiA-KaiC complex with full-length proteins combined with an analysis of KaiC truncation mutants, showed that KaiA binds exclusively to the CII half of KaiC (Pattanayek et al. 2006), suggesting that the previous observation of KaiC binding to the linker region might have been an artifact of yeast two-hybrid interaction methodology .

The last several years have also witnessed a flurry of functional advances in the cyanobacterial circadian clock field (Kageyama et al. 2006; Mori et al. 2007; Ito et al.

2007; Nishiwaki et al. 2007; Rust et al. 2007; Terauchi et al. 2007). Despite the wealth of recent structural and functional data on the KaiABC clock, mysteries regarding its inner workings still remain (Golden et al. 2007). This chapter will provide a detailed account of the anatomy of the *S. elongatus* KaiC hexamer based on the crystal structure obtained at 2.8 Å resolution (Pattanayek et al. 2004). We will also summarize insights obtained regarding the KaiA-KaiC interaction based on our own studies, combining X-ray, crystallography, EM, and modeling (Pattanayek et al. 2006; Mori et al. 2007).

2. Overall structure of KaiC

The crystal structure of *S. elongatus* KaiC determined at 2.8 Å resolution revealed a hexamer in the form of a double doughnut with a constricted waist region and overall dimensions of ca. 100 x 100 Å (**Figure 1C**) (Pattanayek et al. 2004). The central channel of the hexamer is ca. 20 Å wide on average, but the channel is constricted at the CII side by 6 arginine residues (**Figure 2**). The two hexameric rings, CI and CII, have similar overall shapes, but the CII side of the hexamer differs in that it has protruding C-terminal peptides (**Figures 2**). In the initial three-dimensional structural model, the last 20 residues of individual KaiC subunits were missing because the C-terminal regions of individual KaiC molecules exhibit considerable conformational flexibility, resulting in poorly defined electron density. The discovery that the C-terminal residues of KaiC are crucial for KaiA binding (Vakonakis and LiWang 2004) prompted us to a carefully inspect the density above the C-terminal dome and incorporate into the model individual C-terminal tails of various lengths (**Figure 1C**). For two of the subunits all C-terminal residues including Ser-519 were built into the electron density (Pattanayek et al. 2006). Twelve ATP molecules are bound between individual subunits, six each in the N- and C-terminal rings. ATP molecules are almost completely buried in the space between neighboring subunits; only an edge of the adenine base is exposed on the surface of the hexamer (**Figure 2D**).

The KaiC protein is the product of a gene duplication (Ishiura et al. 1998) and the 3D-structure mirrors characteristics at the gene and primary sequence levels in that the KaiC monomer exhibits a two-domain fold (**Figure 3B**). The N-terminal CI and C-terminal CII domains are arranged in a serial fashion and are related by a translation of 42

Å and a rotation of 15°. They adopt fairly similar core structures with an r.m.s. deviation of 2.45 Å based on 208 matching Cα pairs. Notable deviations in the structures of CI and CII are found in their N-terminal and C-terminal regions. In the case of CI, the N-terminal region protrudes from the outer side of the domain and the positions of the first 14 residues were not resolved in electron density maps. Whereas the C-terminal tails of CII jut out from the dome region, following an S-shaped loop that borders on the channel exit, the C-terminal portion of CI links the two domains (**Figure 3D**). Following a short β-strand that is part of the waist, the linker winds up on the outside of the CII domain and enters it near the border of the dome (**Figure 3C**). The existence of this lever-like arrangement suggests an inherent flexibility in the relative orientation of the CI and CII domains. The covalent linkage between CI and CII is required for proper function of the clock. Using the full-length KaiC protein from *T. elongatus* and separately expressed CI and CII domains, it was shown that the combination of the two domains in the absence of the linker led to a drastic reduction in the thermodynamic stability relative to that of the wild-type protein (Hayashi et al. 2006).

As expected from comparisons of the primary sequences that implicated KaiCI and KaiCII as members of the DnaB/RecA superfamily of proteins (Leipe et al. 2000), the structures of the CI and CII cores display similarity to the folds adopted by DNA helicases (Pattanayek et al. 2004). However, comparison of the CI and CII hexameric rings with the hexamers of helicases demonstrates that the similarities are much closer at the monomer level, i.e. ring diameter and locations of the ATP binding cleft differ considerably in some cases. Moreover, none of the helicases features covalently linked rings as seen with KaiC. Unexpectedly, based on sequence alignments, F1 ATPase, a single ring comprised of a trimer of αβ-heterodimers (Abrahams et al. 1994), was found to exhibit the closest structural similarity to the CI and CII hexameric rings (Pattanayek et al. 2004).

3. ATP binding and relative stability of the CI and CII hexamers

ATP molecules are bound between individual subunits in both the CI and CII halves of the KaiC hexamer (**Figure 2**). Note that the crystal structure features the more slowly hydrolyzing ATPγS analog. In both the CI and CII domains of KaiC, ATP forms specific

interactions with the two neighboring subunits. In the CI half contacts to ATP phosphate groups from one monomer include the conserved P-loop amino acids T50, K52 and T53. Residues S89, K232 and D241 form hydrogen bonds to the nucleobase. Residues from the second monomer stabilizing ATP comprise K224 and R226 that contact the γ-phosphate group and H230 that is engaged in a hydrogen bond to the 2'-hydroxyl group of the ribose moiety. The observed binding mode involving P-loop residue K52 is in line with the earlier observation that this lysine is indispensable for ATP binding (Nishiwaki et al. 2000). In addition, the specific interactions made to the nucleobase portion of ATP help rationalize the preference for ATP over GTP by KaiCI. Interestingly, these interactions between CI residues and adenine atoms are missing in the CII half: no direct contacts between amino acid side chains and the nucleobase exist there. This provides a rationalization why KaiCII is unable to discriminate to a significant degree between ATP and GTP (Nishiwaki et al. 2000; Mori and Johnson 2001). Another difference between the CI and CII halves concerns the effect of the mutation of the P-loop lysine: the KaiCI K52H mutant triggered a complete disruption of the rhythm whereas mutation of the corresponding CII K294 to histidine resulted in a long-period phenotype (Nishiwaki et al. 2000). The structure reveals that unlike K52, K294 does not engage in a direct contact to the ATP γ-phosphate. Instead of K294 another lysine, K457, forms a salt bridge to that phosphate group. On the other hand threonines from the Walker A motif (T53 in CI and T295 in CII) interact with the γ-phosphate of ATP directly or via Mg^{2+} (T295) in both halves, thus explaining the arhythmic phenotype of T53A and T295A mutants (Mori and Johnson 2001).

The crystal structure revealed different binding modes for ATP in the CI and CII halves. The binding interface in CI is specific for ATP (due to direct interactions with the nucleobase), but a conformational disorder of the γ-phosphate group in CI evident in electron density maps supports the notion that this portion of ATP is rather loosely bound. Conversely, the CII binding interface manifests only weak restraints of the nucleobase portion, whereas the γ-phosphate is tightly gripped by surrounding residues as well as Mg^{2+}. That these observations regarding differences between ATP binding and subunit interfaces in the CI and CII halves are not simply artifacts of the crystal structure is corroborated by thermodynamic data that indicate that the CI ring is more stable than

the CII ring. This finding is essential as it implies different functions of the CI and CII rings.

4. Subunit interface and phosphorylation

KaiC is an auto-kinase that phosphorylates serines and threonines as well as an auto-phosphatase, and it exhibits both of these functions in vitro and in vivo (Nishiwaki et al. 2000; Iwasaki et al. 2002; Xu et al. 2003) and clock speed is correlated with the level of phosphorylation (Xu et al. 2003). Expression in *E. coli* and purification of the KaiC protein from *S. elongatus* are always carried out in the presence of ATP. Therefore, the resultant protein is a mixture of the phospho- and dephospho-forms as judged by SDS-PAGE analysis. Although ATP was replaced by ATPγS prior to crystallization, the crystal structure could thus be expected to disclose phosphorylation sites. Following refinement of the crystal structure, inspection of difference Fourier electron density maps revealed peaks in the vicinity of two residues, T432 and S431 that are consistent with the presence of phosphate groups (Pattanayek et al. 2004; Xu et al. 2004) (**Figure 4**). In the crystal structure, the threonine is phosphorylated in all six subunits and serine is phosphorylated in four subunits. A second threonine, T426 is located in the immediate vicinity of S431 and its hydroxyl group forms a hydrogen bond to the phosphate of the latter. However, T426 does not seem to become phosphorylated.

Individual T432A and S431A mutations and also the T426A mutation alter KaiC phosphorylation in vivo (Xu et al. 2004). Both the T432A and T426A mutations lead to a significant reduction in the amount of phosphorylated KaiC. On the other hand, the S431A mutation increases the ratio of phospho-KaiC to dephospho-KaiC. The S431A/T426A double mutant displays phosphorylation that is similar to that of wild-type KaiC and the triple mutant T432A/S431A/T426A shows no sign of phosphorylation. This latter observation and the lack of phosphorylation with the T432A/S431A double mutant (Nishiwaki et al. 2004) provide evidence that there are two main phosphorylation sites per KaiC subunit. The KaiCI domain seems to be devoid of phosphorylatable Ser and The residues. The individual T432A, S431A and T426A mutants abolish circadian rhythmicity and the double and triple mutants are also arhythmic. The effect does not

seem related to the inability of phosphorylation mutants to hexamerize as the mutations do not disrupt hexamer formation (Xu et al. 2004).

Residues T432, S431 and T426 are located in a loop region that connects two β strands and the two latter residues face each other across the loop (**Figure 4**). A Mg^{2+} ion coordinates to the β- and γ-phosphate groups of ATP and engages in additional inner-sphere contacts to the side chains of residues T295, E318, E319 and D378 from a subunit adjacent to that carrying phosphorylated T432 and S431 residues. Hence, KaiC phosphorylation proceeds across the subunit interface and the presence of phosphate groups at T432 and S431 results in additional interactions between amino acids from neighboring subunits. Phosphorylation of T432 leads to new contacts to R385 and E318 from the adjacent subunit. In the case of S431 addition of a phosphate results in a hydrogen bond to H429 from the same subunit. This histidine in turn interacts with D427 from the adjacent subunit. An additional interaction of the S431 phosphate concerns the previously described hydrogen bond to the γ-hydroxyl group of T426, a contact that is absent in the dephospho-KaiC structure. Based on the analysis of the interactions at the subunit interfaces in the phospho-KaiC hexamer, it would appear that phosphorylation of T432 and S431 leads to tighter binding between adjacent CII domains.

Recently it was shown that the phosphorylation cycle of the KaiC protein entails four steps - T432 phosphorylation, S431 phosphorylation, T432 dephosphorylation and S431 dephosphorylation - and that the product of each step regulates the reaction in the next step (Nishiwaki et al. 2007; Rust et al. 2007). Complete phosphorylation of both T432 and S431 converts KaiC from an auto-kinase to an auto-phosphatase. The finding that T432 is the first site to be phosphorylated is consistent with the crystallographic data that revealed phosphorylated T432 residues in all six subunits (only four of the six S431 residues were phosphorylated). Although all T432 and S431 residues are relatively far removed from the γ-phosphate of ATP, the distances between the T432 hydroxyl groups and the γ-phosphates are shorter on average (7.1 Å for Chain A) than those between the S431 hydroxyl groups and the γ-phosphates (8.2 Å for Chain A; **Figure 4**). Phosphorylation of T432 generates new contacts across subunit interfaces (i.e. the interaction to E318) that could in turn lead to increased phosphorylation of S431. The hexamer trapped in the crystal structure is likely representative of the

hyperphosphorylated form of KaiC. The distances between the hydroxyl groups of both T432 and S431 and the γ-phosphate of ATP exceed by far the spacing consistent with an active form of the kinase. This points to a considerable plasticity of the interface between CII domains, a notion that is in line with the different functions of the KaiCI and KaiCII halves inferred above from divergent ATP binding and thermodynamic stabilities as well as the fact that the CI half lacks phosphorylation sites. It is reasonable to view the CI ring as a structural platform with a relatively rigid interface between subunits. Conversely, the CII ring is composed of subunits with variable relative orientations - most likely the result of small conformational adjustments in the central linker region between CI and CII - that form the basis for the controlled step-by-step phosphorylation and dephosphorylation process with a concomitant transition of KaiC from an auto- kinase to an auto-phosphatase.

5. The KaiA-KaiC interaction

5.1 Binding of the KaiA dimer to the C-terminal tail of KaiC

Overexpression of KaiA results in enhancement of *kaiBC* promoter activity, while continuous high-levels of KaiC results in repression of the *kaiBC* promoter (Ishiura et al., 1998). Both in vitro and in vivo, KaiA is an enhancer of KaiC phosphorylation and KaiB antagonizes the action of KaiA (Iwasaki et al., 2002; Williams et al., 2002; Kitayama et al., 2003; Xu et al., 2003). In the case of *T. elongatus* it was found that a single KaiA dimer is sufficient to upregulate the phosphorylation of a KaiC hexamer to saturated levels (Hayashi et al. 2004b), consistent with the higher abundance of KaiC in vivo relative to KaiA (Kitayama et al. 2003). It is noteworthy that the question whether KaiA actually increases phosphorylation or decreases dephosphorylation is still open at the moment. Early models had placed the KaiA-KaiC binding interface in the waist region of the KaiC double hexamer (Vakonakis et al. 2004; Taniguchi et al. 2001). The models by Taniguchi and coworkers relied on yeast two-hybrid screens of KaiA with fragments of KaiC. KaiA exhibited affinities to C-terminal fragments from CI and CII that were not drastically reduced compared to that for the full-length KaiC protein. Prior to the crystal structure of KaiC, it was believed that the CII domain might fold back onto the CI domain, resulting in a tail-to-tail orientation of the two halves. The C-terminal regions

implicated in KaiA binding would then map to the central waist region. However, the crystal structure demonstrated that CI and CII are arranged head-to-tail (**Figure 1**). Thus, the KaiA-binding regions based on the two-hybrid analysis would be located at the waist and the CII-terminal dome and therefore be far removed from one another. An alternative theoretical model had the refolded KaiA dimer inserted into the central channel of KaiC (Wang, 2005). Neither model is consistent with more recent biochemical and structural data.

Vakonakis and LiWang determined the NMR solution structure of the complex between the C-terminal domain of *T. elongatus* KaiA (residues 180–283) and a 30mer peptide (residues 488-518) derived from the C-terminus of *T. elongatus* KaiC (Vakonakis and LiWang 2004) (**Table 4**). Unlike the C-terminal region of KaiCII for which a specific interaction with the dimer of the C-terminal domain of KaiA was found, a KaiCI C-terminal peptide corresponding to residues 241–260 of *T. elongatus* KaiC when mixed with KaiA did not trigger any changes in the NMR spectra of the latter. The conformation of the dimerized C-terminal domain of KaiA does not fundamentally alter upon binding to two KaiC peptides. Thus, the overall fold of KaiA with the four α-helices organized into two antiparallel helix–loop–helix pairs is maintained in the complex (**Figure 5**). KaiA molecules dimerize along the C-terminal half of the longest α-helix, primarily via coiled-coil hydrophobic interactions. The dimer interface is stabilized by additional hydrophobic interactions and an inter-subunit salt bridge as well as two putative hydrogen bonds. The relatively wide angle of around 50° between pairs of antiparallel α-helices at the dimerization interface of KaiA opens up somewhat as a consequence of binding of KaiC peptides. Whereas the KaiA monomeric subunit is more or less unchanged by KaiC-peptide binding, the angle of dimerization changes between free and bound KaiA through a relative rotation around the dimerization interface. This rotation is due to the KaiC peptides inserting non-polar side chains of residues L505 and A506 into the KaiA dimerization groove, thereby forming a hydrophobic cluster with side chains of KaiA residues L233, H236, L264 and I265. It has been suggested that the KaiA-KaiC affinity can be modulated by changes in the dimerization geometry of the KaiA C-terminal domain (Vakonakis and LiWang 2004). The backbone r.m.s. deviation between the structures of free and bound KaiA dimers amounts to about 1.3 Å including all

ordered residues. C-terminal KaiCII peptides bound to the KaiA dimer adopt an extended L-shaped conformation (**Figure 5**). Beginning at the N-terminus, peptides cross the helix–loop–helix pair of one KaiA C-terminal subunit and then, after a turn, follow the groove between KaiA subunits. Because individual KaiC peptides engage in extensive contacts to both KaiA subunits, KaiA dimerization is a prerequisite for KaiC binding. Binding of KaiC peptides involves a combination of hydrophobic, electrostatic, and hydrogen bonding interactions with KaiA (Vakonakis and LiWang 2004).

5.2 Electron microscopy studies

We carried out a negative-stain electron microscopic analysis of the *T. elongatus* KaiA-KaiC complex using full-length proteins (Pattanayek et al. 2006). Under the conditions used, only 1:1 KaiA dimer:KaiC hexamer complexes were observed. Although it is possible that two (Hayashi et al, 2004b) KaiA dimers are bound to KaiC, this is unlikely to occur in vivo because the concentration of KaiC molecules in the cell far exceeds that of KaiA (Kitayama et al. 2003; Johnson and Egli 2004). And, as stated above, one KaiA dimer was sufficient to saturate KaiC phosphorylation. A 1:1 stoichiometry was subsequently also found for the KaiA-KaiC complex from *S. elongatus* in a time-dependent analysis of the interactions between Kai proteins employing negative-stain EM, native gels and fluorescence (Mori et al. 2007). Electron micrographs show the KaiA dimer protruding from the dome surface at one end of the KaiC hexamer particle (**Figure 6**). Native PAGE of mixtures of KaiA either with wild-type KaiC or a C-terminal deletion mutant lacking the last 25 residues demonstrated that the lack of the C-terminal tail prevents binding by KaiA (Pattanayek et al. 2006). A C-terminal deletion in KaiC also abolishes rhythmicity in vivo, but not hexamerization in vitro. An EM study of KaiA mixed with a truncated form of KaiC also showed no evidence of complex formation without the C-terminal residues. These observations are consistent with the observation by Vakonakis and LiWang that the KaiA dimer specifically recognizes the C-terminal KaiCII peptide and indicates that KaiA probably contacts only the CII half.

Electron microscopy revealed that the KaiA dimer assumes various orientations vis-à-vis the CII dome surface (**Figure 6**). In the crystal structure of full-length *S. elongatus* KaiC, C-terminal peptides from the six subunits exhibited various

conformations, one of which resembles that of the model peptide in the NMR structure of the KaiA dimer-KaiC peptide complex. Given the flexibility of the C-terminal region the range of orientations observed for the KaiA dimer bound to KaiC is not surprising. However, EM images of the KaiA-KaiC complex also reveal that the KaiA dimer is at some distance (~35 Å) from the hexameric barrel of KaiC. This suggests that the KaiC S-shaped loop bordering on the channel at the surface of the CII dome may become unraveled and pulled out upon binding of KaiA (**Figure 5C** and **D**). An EM reconstruction of the KaiA-KaiC complex reveals two plumes of weak density extending from one end of the KaiC hexameric barrel (**Figure 6B**). These plumes extend in two directions and suggest that KaiA is not bound to KaiC in a single defined orientation, but rather KaiA occupies a variety of positions relative to the main barrel of KaiC. Using the EM reconstruction of the KaiA-KaiC complex as a guide, models of "tethered" and "engaged" KaiA-KaiC complexes were built (**Figures 7A** and **B**) (Pattanayek al. 2006). Given the limited resolution of ~24 Å of the EM structure, a more detailed model of the KaiA-KaiC complex cannot be built. However it is clear that some region near the C-terminus of KaiC must serve as a flexible linker between the KaiA dimer and the KaiC hexameric barrel. On the basis of these models, we postulated that the engaged mode might enable a secondary contact between the apical loop of one KaiA monomer and the region between two KaiC subunits harboring ATP. A contact involving this region of KaiA is consistent with the effects of mutations of individual loop residues on the period of the clock (Ye et al. 2004). For example, KaiA residues could interact with KaiCII residues surrounding the ATP cleft and thus affect the inter-subunit phosphorylation activity (Pattanayek et al 2004; Xu et al. 2004). Alternatively, covering the ATP cleft could simply enhance the residence time of ATP thus resulting in an enhancement of phosphorylation. This would be consistent with direct measurements of the dephosphorylation rate of turnover (Xu et al. 2003).

6. Summary and outlook

A decade after the *kaiA*, *kaiB* and *kaiC* genes were shown to be essential for proper circadian function in the model organism *S. elongatus* (Ishiura et al. 1998), the KaiABC clock has now become the best characterized clock system at the molecular level. This is

to some extent due to the remarkable finding that a circadian oscillator can be reconstituted in vitro from the KaiA, KaiB and KaiC proteins in the presence of ATP (Nakajima et al. 2005). Major advances have been made in terms of the functional and structural characterization of the clock in recent years. A possible view of the cyanobacterial circadian clock as consisting of single KaiC particles associating with KaiA and KaiB to different extents over the daily cycle has given way to a model based on a dynamic equilibrium entailing different types of complexes whose concentrations oscillate with a period of ca. 24 hours (Kageyama et al. 2006; Mori et al. 2007). Thus, free KaiC hexamers coexist with KaiCs bound to KaiA or KaiB or both. KaiC in these complexes exhibits alternative phosphorylation states and during a single 24 h cycle, KaiC progresses from the hypo- to the hyper-phosphorylated and back to the hypo-phosphorylated state.

Three-dimensional structures for all three proteins have been available for some time but high-resolution structures of complexes are still elusive. The crystal structure of the KaiC hexamer provided a wealth of information on the architecture and conformational underpinnings of the central cog (Pattanayek et al. 2004). Phosphorylation sites were readily discernible in electron density maps (Xu et al. 2004) and the T432 and S431 sites (Nishiwaki et al. 2007; Rust et al. 2007) were phosphorylated in the crystal structure of KaiC. The structure and subsequent analyses of KaiA-KaiC interactions using solution NMR (Vakonakis and LiWang 2004), biochemical (Hayashi et al. 2004ab) and hybrid structural approaches including EM (Pattanayek et al. 2006) also demonstrated different functions of the CI and CII domains of KaiC. Thus, the CI hexamer serves as a structural platform and the CII hexamer is conformationally more flexible and harbors all phosphorylation sites as well as the kinase and phosphatase activities.

Although the combined structural and functional data have provided important insights on the possible mechanisms of the control of KaiC phosphorylation by KaiA and the kinase activity of KaiC, there is an urgent need to gain a better understanding of the conformational changes in KaiC that underlie the switch from the kinase (endpoint hyper-phosphorylated state) to the phosphatase activity (endpoint hypo-phosphorylated state) (Nishiwaki et al. 2007). Although it is now reasonably clear that both KaiA and KaiB

interact with the C-terminal CII domains [see also our recent paper on the model of the binary KaiB-KaiC complex (Pattanayek et al. 2008)], the lack of high-resolution structures of binary and ternary complexes of KaiC and structures of KaiC hexamers or mutants trapped in different phosphorylation states constitutes a bottleneck on the road to a complete mechanistic dissection of the KaiABC clock. Crystal structure determinations for KaiCs of various phosphorylation states and a range of complexes are important near-term goals of research concerning the *S. elongatus* KaiABC clock. A further problem of central importance concerns the molecular basis of temperature compensation. Because the in vitro KaiABC timer is temperature compensated, it stands to reason that combined biochemical and biophysical analyses will eventually uncover the molecular origins of this salient property of all circadian clocks. Long-term goals also concern a structural characterization of the interactions between the minimal components of the circadian oscillator and mediators of input [i.e. the histidine kinase CikA (Schmitz et al. 2000)] and output signals [i.e. the histidine kinase SasA (Iwasaki et al. 2000)], the latter pathway including those that regulate the general transcription mechanism (Tomita et al. 2005).

References

Abrahams JP, Leslie AGW, Lutter R, Walker JE (1994) Structure at 2.8 Å resolution of F1 ATPase from bovine heart mitochondria. Nature 370:621-628

Berman HM, Westbrook J, Feng Z, Gilliland G, Bhat TN, Weissig H, Shindyalov IN, Bourne PE (2000) The Protein Data Bank. Nucleic Acids Res 28:235-242

Egli M, Pattanayek R, Pattanayek S (2007) Protein-protein interactions in the cyanobacterial KaiABC circadian clock. In: Boeyens JCA, Ogilvie JF (eds) Models, Mysteries, and Magic of Molecules; Proceedings of the INDABA-5 Conference, Kruger National Park, South Africa, August 20-25, 2006, Springer Publishers, Dordrecht, The Netherlands, pp 287-303

Garces RG, Wu N, Gillon W, Pai EF (2004) Anabaena circadian clock proteins KaiA and KaiB reveal potential common binding site to their partner KaiC. EMBO J 23:1688-1698

Golden SS (2004) Meshing the gears of the cyanobacterial circadian clock. Proc Natl Acad Sci USA 101:13697-13698

Golden SS, Cassone VM, LiWang A (2007) Shifting nanoscopic clock gears. Nat Struct Mol Biol 14:362-363

Hayashi F, Suzuki H, Iwase R, Uzumaki T, Miyake A, Shen J-R, Imada K, Furukawa Y, Yonekura K, Namba K, Ishiura M (2003) ATP-induced hexameric ring structure of the cyanobacterial circadian clock protein KaiC. Genes to Cells 8:287-296

Hayashi F, Itoh N, Uzumaki T, Iwase R, Tsuchiya Y, Yamakawa H, Morishita M, Onai K, Itoh S, Ishiura M (2004a) Roles of two ATPase-motif-containing domains in cyanobacterial circadian clock protein KaiC. J Biol Chem 50**:**52331-52337

Hayashi F, Ito H, Fujita M, Iwase R, Uzumaki T, Ishiura M (2004b) Stoichiometric interactions between cyanobacterial clock proteins KaiA and KaiC. Biochem Biophys Res Comm 316:195-202

Hayashi F, Iwase R, Uzumaki T, Ishiura M (2006) Hexamerization by the N-terminal domain and intersubunit phosphorylation by the C-terminal domain of cyanobacterial circadian clock protein KaiC. Biochem Biophys Res Comm 318:864-872

Hitomi K, Oyama T, Han S, Arvai AS, Getzoff ED (2005) Tetrameric architecture of the circadian clock protein KaiB: a novel interface for intermolecular interactions and its impact on the circadian rhythm. J Biol Chem 280:18643-18650

Ishiura M, Kutsuna S, Aoki S, Iwasaki H, Andersson CR, Tanabe A, Golden SS, Johnson CH, Kondo T (1998) Expression of a gene cluster *kaiABC* as a circadian feedback process in cyanobacteria. Science 281:1519-1523

Ito H, Kageyama H, Mutsuda M, Nakajima M, Oyama T, Kondo T (2007) Autonomous synchronization of the circadian KaiC phosphorylation rhythm. Nat Struct Mol Biol 14:1084-1088

Iwasaki H, Williams SB, Kitayama, Y, Ishiura M, Golden SS, Kondo T (2000) A kaiC-interacting sensory histidine kinase, SasA, necessary to sustain robust circadian oscillation in cyanobacteria. Cell 101:223-233.

Iwasaki H, Nishiwaki T, Kitayama Y, Nakajima M, Kondo T (2002) KaiA-stimulated KaiC phosphorylation in circadian timing loops in cyanobacteria. Proc Natl Acad Sci USA 99:15788-15793

Iwase R, Imada K, Hayashi F, Uzumaki T, Morishita M, Onai K, Furukawa Y, Namba K, Ishiura M (2005) Functionally important substructures of circadian clock protein KaiB in a unique tetramer complex. J Biol Chem 280:43141-43149

Johnson CH, Egli M (2004) Visualizing a biological clockwork's cogs. Nat Struct Mol Biol 11:584-585

Kageyama H, Nishiwaki T, Nakajima M, Iwasaki H, Oyama T, Kondo T (2006) Cyanobacterial circadian pacemaker: Kai protein complex dynamics in the KaiC phosphorylation cycle in vitro. Mol Cell 23:161-171

Kitayama Y, Iwasaki H, Nishiwaki T, Kondo T (2003) KaiB functions as an attenuator of KaiC phosphorylation in the cyanobacterial circadian clock system. EMBO J 22:1-8

Leipe DD, Aravind L, Grishin NV, Koonin EV (2000) The bacterial replicative helicase DnaB evolved from a RecA duplication. Genome Res 10:5-16

Mori T, Johnson CH (2001) Circadian programming in cyanobacteria. Sem. Cell Develop. Biol. 12:271-278

Mori T, Saveliev SV, Xu Y, Stafford WF, Cox MM, Inman RB, Johnson, CH (2002) Circadian clock protein KaiC forms ATP-dependent hexameric rings and binds DNA.

Proc Natl Acad Sci USA 99:17203-17208

Mori T, Williams DR, Byrne M, Qin X, Egli M, Mchaourab H, Stewart PL, Johnson CH (2007) Elucidating the ticking of an in vitro circadian clockwork. PLOS Biol 5:841-853

Nakajima M, Imai K, Ito H, Nishiwaki T, Murayama Y, Iwasaki H, Oyama T, Kondo T (2005) Reconstitution of circadian oscillation of cyanobacterial KaiC phosphorylation in vitro. Science 308**:**414-415

Nishiwaki T, Iwasaki H, Ishiura M, Kondo T (2000) Nucleotide binding and autophosphorylation of the clock protein KaiC as a circadian timing process of cyanobacteria. Proc Natl Acad Sci USA 97:495-499

Nishiwaki T, Satomi Y, Nakajima M, Lee C, Kiyohara R, Kageyama H, Kitayama Y, Temamoto M, Yamaguchi A, Hijikata A, Go M, Iwasaki H, Takao T, Kondo T (2004) Role of KaiC phosphorylation in the circadian clock system of *Synechococcus elongatus* PCC 7942. Proc Natl Acad Sci USA 101**:**13927-13932

Nishiwaki T, Satomi Y, Kitayama Y, Terauchi K, Kiyohara R, Takao T, Kondo T (2007) A sequential program of dual phosphorylation of KaiC as a basis for circadian rhythm in cyanobacteria. EMBO J 26:4029-4037

Pattanayek R, Wang J, Mori T, Xu Y, Johnson CH, Egli M (2004) Visualizing a circadian clock protein: crystal structure of KaiC and functional insights. Mol Cell 15:375-388

Pattanayek R, Williams DR, Pattanayek S, Xu Y, Mori T, Johnson CH, Stewart PL, Egli M (2006) Analysis of KaiA-KaiC protein interactions in the cyanobacterial circadian clock using hybrid structural methods. EMBO J 25:2017-2038

Pattanayek R, Williams DR, Pattanayek S, Mori T, Johnson CH, Stewart PL, Egli M (2008) Structural model of the circadian clock KaiB-KaiC complex and mechanism for modulation of KaiC phosphorylation. EMBO J 27:1767-1778

Pettersen EF (2004) UCSF Chimera - a visualization system for exploratory research and analysis. J Comput Chem 25:1605-1612

Rust MJ, Markson JS, Lane WS, Fisher DS, O'Shea EK (2007) Ordered phosphorylation governs oscillation of a three-protein circadian clock. Science 318:809-812

Schmitz O, Katayama M, Williams SB, Kondo T, and Golden SS (2000) CikA, a bacteriophytochrome that resets the cyanobacterial circadian clock. Science 289:765-

768

Taniguchi Y, Yamaguchi A, Hijikata A, Iwasaki H, Kamagata K, Ishiura M, Go M, Kondo T (2001) Two KaiA-binding domains of cyanobacterial circadian clock protein KaiC. FEBS Lett 496:86-90

Terauchi K, Kitayama Y, Nishiwaki T, Miwa K, Murayama Y, Oyama T, Kondo T (2007) The ATPase activity of KaiC determines the basic timing for circadian clock in cyanobacteria. Proc Natl Acad Sci USA 104:16377-16381

Tomita J, Nakajima M, Kondo T, Iwasaki H (2005) Circadian rhythm of KaiC phosphorylation without transcription-translation feedback. Science 307:251-254

Uzumaki T, Fujita M, Nakatsu T, Hayashi F, Shibata H, Itoh N, Kato H, Ishiura M (2004) Crystal structure of the C-terminal clock-oscillator domain of the cyanobacterial KaiA protein. Nat Struct Mol Biol 11:623-631

Vakonakis I, Sun J, Wu T, Holzenburg A, Golden SS, LiWang AC (2004a) NMR structure of the KaiC-interacting C-terminal domain of KaiA, a circadian clock protein: Implications for the KaiA-KaiC Interaction. Proc Natl Acad Sci USA 101:1479-1484

Vakonakis I, LiWang AC (2004) Structure of the C-terminal domain of the clock protein KaiA in complex with a KaiC-derived peptide: implications for KaiC regulation. Proc Natl Acad Sci USA 101:10925-10930

Vakonakis I, Klewer DA, Williams SB, Golden SS, LiWang AC (2004b) Structure of the N-terminal domain of the circadian clock-associated histidine kinase SasA. J Mol Biol 342:9-17

Wang J (2005) Recent cyanobacterial Kai protein structures suggest a rotary clock. Structure 13:735-741

Williams SB, Vakonakis I, Golden SS, LiWang AC (2002) Structure and function from the circadian clock protein KaiA of *Synechococcus elongatus*: a potential clock input mechanism. Proc Natl Acad Sci USA 99:15357-15362

Xu Y, Mori T, Johnson CH (2003) Cyanobacterial circadian clockwork: roles of KaiA, KaiB, and the *kaiBC* promoter in regulating KaiC. EMBO J 22:2117-2126

Xu Y, Mori T, Pattanayek R, Pattanayek S, Egli M, Johnson CH (2004) Identification of key phosphorylation sites in the circadian clock protein KaiC by crystallographic and

mutagenetic analyses. Proc Natl Acad Sci USA 101:13933-13938

Ye S, Vakonakis I, Ioerger TR, LiWang AC, Sacchettini JC (2004) Crystal structure of circadian clock protein KaiA from *Synechococcus elongatus*. J Biol Chem 279:20511-20518

Tables

Table 1. Three-dimensional structures of protein KaiA

Protein	Construct	Organism	Technique	Reference	PDB ID code[a]
KaiA	N-terminal domain	PCC7942 *Synechococcus elongatus* (*S. elongatus*)	NMR	Williams et al. 2002	1M2E
KaiA	full-length	*S. elongatus*	X-ray	Ye et al. 2004	1R8J
KaiA	full-length	PCC7120 *Anabaena (Anabaena)*	X-ray	Garces et al. 2004	1R5Q
KaiA	C-terminal domain	*Thermosynechococcus elongatus* BP-1 (*T. elongatus*)	X-ray	Uzumaki et al. 2004	1V2Z
KaiA	C-terminal domain	*T. elongatus*	NMR	Vakonakis et al. 2004a	1Q6A

[a] http://www.rcsb.org (Berman et al. 2000)

Table 2. Three-dimensional structures of protein KaiB

Protein	Construct	Organism	Technique	Reference	PDB ID code
KaiB	full-length	*Anabaena*	X-ray	Garces et al. 2004	1R5P
KaiB	full-length	PCC6803 *Synechocystis*	X-ray	Hitomi et al. 2005	1WWJ
KaiB	full-length (T64C mutant)	*T. elongatus*	X-ray	Iwase et al. 2005	1VGL
KaiB	full-length (wild type)	*T. elongatus*	X-ray	Pattanayek et al. 2008	2QKE

Table 3. Three-dimensional structures of protein KaiC

Protein	Construct	Organism	Technique	Reference	PDB ID code
KaiC	full-length	*S. elongatus*	X-ray	Pattanayek et al. 2004	1TF7
KaiC	full-length; the structure is based on the same cryst-allographic data as 1TF7, but phosphate groups were added to S431 (in 4 subunits) and T432 (in 6 subunits)	*S. elongatus*	X-ray	Xu et al. 2004	1U9I
KaiC	full-length; the structure is based on the same cryst-allographic data as 1TF7, but the C-terminal tails of subunits were extended to varying degrees and for two of them all residues up to S519 were added	*S. elongatus*	X-ray	Pattanayek et al. 2006	2GBL

Table 4. Three-dimensional structures of KaiA-KaiC complexes

Protein	Construct	Organism	Technique	Reference	PDB ID code
KaiA/KaiC	C-terminal KaiC peptide (amino acids 488-518), in complex with the C-terminal domain of KaiA	*T. elongatus*	NMR	Vakonakis and LiWang 2004	1SUY
KaiA/KaiC	full-length KaiA and KaiC; the complex was modeled using coordinates of the crystal structures of KaiC (2GBL) and KaiA (1R8J) and the KaiC peptide-KaiA complex (1SUY) from NMR	*T. elongatus*	EM	Pattanayek et al. 2006	—

Figures

Figure 1. Structures of the cyanobacterial clock proteins KaiA, KaiB, and KaiC. (A) The crystal structure of the *S. elongatus* KaiA dimer, molecular mass ~64 kDa (PDB-ID 1R8J) (Ye et al. 2004). (B) The crystal structure of the *Synechocystis* KaiB tetramer, molecular mass ~48 kDa (PDB-ID 1WWJ) (Hitomi et al. 2005). (C) The crystal structure of the *S. elongatus* KaiC hexamer with extended C-termini, molecular mass ~360 kDa (PDB-ID 2GBL) (Pattanayek et al. 2006). Each subunit of the multimeric proteins (KaiA, KaiB, and KaiC) is colored differently. Molecular graphics image produced with the UCSF Chimera package (Pettersen et al. 2004).

Figure 2. Twelve ATP binding sites in KaiC. (A) There are six ATP binding sites between subunits in the ring of KaiC CI domains. The average diameter of the central channel is 20Å as indicated by the double arrow. View is from the CI surface of the hexamer. (B) There are an additional six ATP binding sites between subunits in the ring of KaiC CII domains. The side chains of Arg488, which constrict the opening of the central channel on the CII side, are shown. View is from the CII surface of the hexamer. (C) Side view of the KaiC hexamer. The CI and CII surfaces are indicated. (D) Enlarged view of boxed region in part C showing one ATP molecule between two CII domains with the tip of the adenine base (blue and white) most accessible and the three phosphate groups (cyan and red) buried within the protein. ATP molecules are shown colored by element type and alternately KaiC subunits are shown in light gray and black (PDB-ID 2GBL).

Figure 3. KaiC is the product of gene duplication. (A) The KaiC hexamer with one of the six subunits (chain A) shown rainbow colored, N-terminus in magenta and C-terminus in red. (B) KaiC chain A with the CI and CII domains indicated and the S-shaped loop (aa485-497) boxed. The N-terminal 13 residues, which extend from the side of the CI domain, are missing due to disorder. Residue E14 (magenta) is shown with its sidechain in ball-and-stick representation. Residue S519 is the C-terminal residue of *S. elongatus* KaiC and it is modeled in two of the six chains (A and F) (PDB-ID 2GBL). (C)

CI domain (aa14-261) including the extended linker between domains (red). The N-terminal residue, E14, is shown with its sidechain (magenta). (D) CII domain (aa262-519) including the flexible C-terminal tail (red). The N-terminal residue, R262, is shown with its sidechain (magenta).

Figure 4. Phosphorylation sites in KaiC. (A) KaiC chain A (light gray) with a short portion of the neighboring chain F (black) including the P-loop (aa288-295) (PDB-ID 2GBL). Also shown are the ATPγS bound between the CII domains (sky blue) and the nearby Mg^{2+} ion (magenta). The chain A T426 (blue), phosphorylated S431 (yellow), and phosphorylated T432 (red), as well as chain F K294 in the P-loop (black), are shown with their sidechains. (B) Enlarged view of the kinase active site with the distances between the S431 and T432 hydroxyl groups with the ATPγS-phosphate indicated by dashed lines (green). These distances are 8.2 and 7.1 Å, respectively.

Figure 5. Interaction of the KaiC C-terminal peptide with KaiA. (A) NMR structure of a complex with a C-terminal KaiC peptide (aa488-518) and the C-terminal domain of KaiA (PDB-ID 1SUY) (Vakonakis and LiWang 2004). Two KaiC peptides are shown in red and blue and the KaiA dimer is shown in light gray and black. There are two roughly perpendicular interaction regions in the KaiC peptide, which correspond to aa490-500 and aa501-510. The first interaction region crosses the apical helix-loop-helix of a KaiA subunit (black), while the second interaction region follows the groove between KaiA subunits. Note the KaiC residue numbers have been adjusted to correspond to the *S. elongatus* sequence. (B) NMR structure with the KaiC S-shaped loop residues (aa485-497) of one chain in red. (C) One KaiC subunit CII domain from the crystal structure (PDB-ID 2GBL) with the S-shaped loop in red, and the remainder of the C-terminal tail in gold. (D) One KaiC subunit CII domain modified to show the S-shaped loop in a modified pulled out conformation with the remainder of the C-terminal tail (aa498-519) in light blue.

Figure 6. Electron microscopy of KaiA-KaiC complex. (A) Individual particle images of negatively stained *T. elongatus* BP-1 KaiA-KaiC (top row) compared to 25 Å filtered

representations of the KaiA (blue) and KaiC (gold) crystal structures. The particle images are shown filtered to 20 Å resolution. (B) EM reconstruction of KaiA-KaiC based on ~4,000 negatively stained particle images. The resolution of the reconstruction is 24 Å. The reconstruction is shown in three views (0°, 45° and 90°) and with two isosurface values. At the lower isosurface two plumes of weak, diffuse KaiA density (indicated by arrows) connect to the KaiC hexameric barrel near the central channel. Scale bars, 100 Å. Reprinted from (Pattanayek et al. 2006).

Figure 7. Tethered and engaged models of the KaiA-KaiC complex. (A) The "tethered" model of the KaiA-KaiC complex with KaiC aa485-500 forming an extended flexible linker between the KaiA dimer and the hexameric barrel of KaiC. In this model KaiA is ~35 Å above the KaiC hexameric barrel, in agreement with EM images of the KaiA-KaiC complex. Note that in this model both the KaiC S-shaped loop (aa485-497) and one of the two KaiC interaction regions (aa490-500) have been extended to form the linker. (B) The "engaged" model of the KaiA-KaiC complex with KaiC aa 485-489 forming a short compact linker. For clarity the S-shaped loops have been removed from all six chains of KaiC. Modified from (Pattanayek et al. 2006).

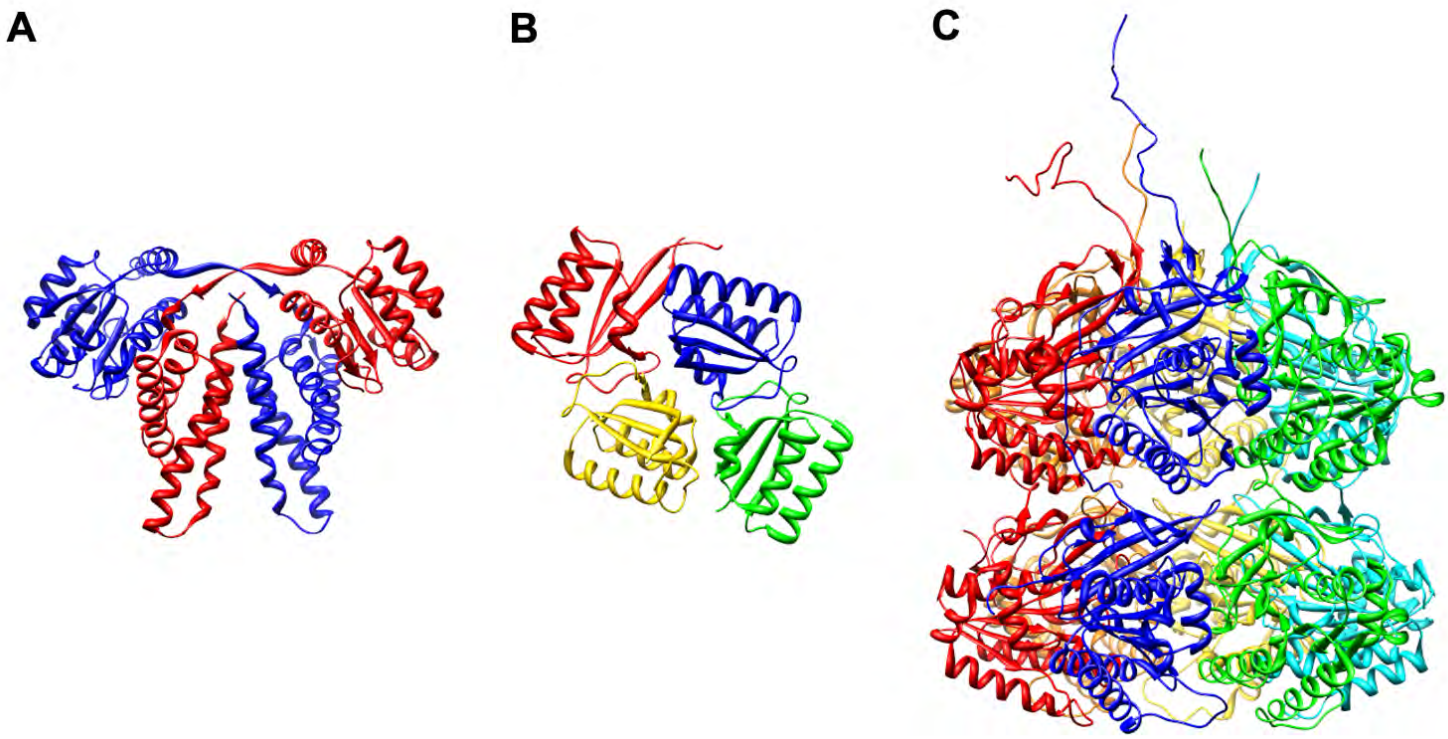
A
B
C

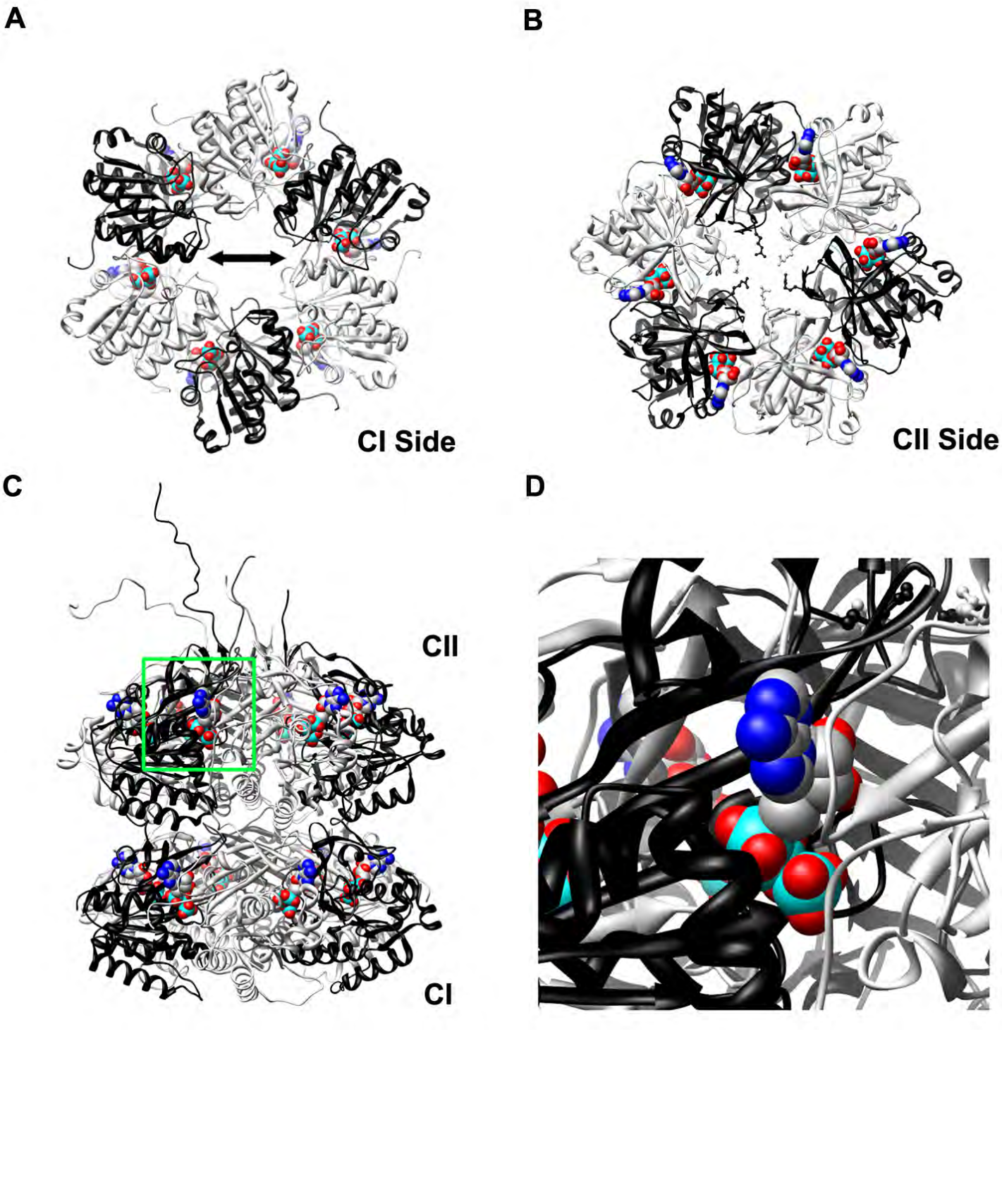
A
CI Side
B
CII Side
C
CII
CI
D

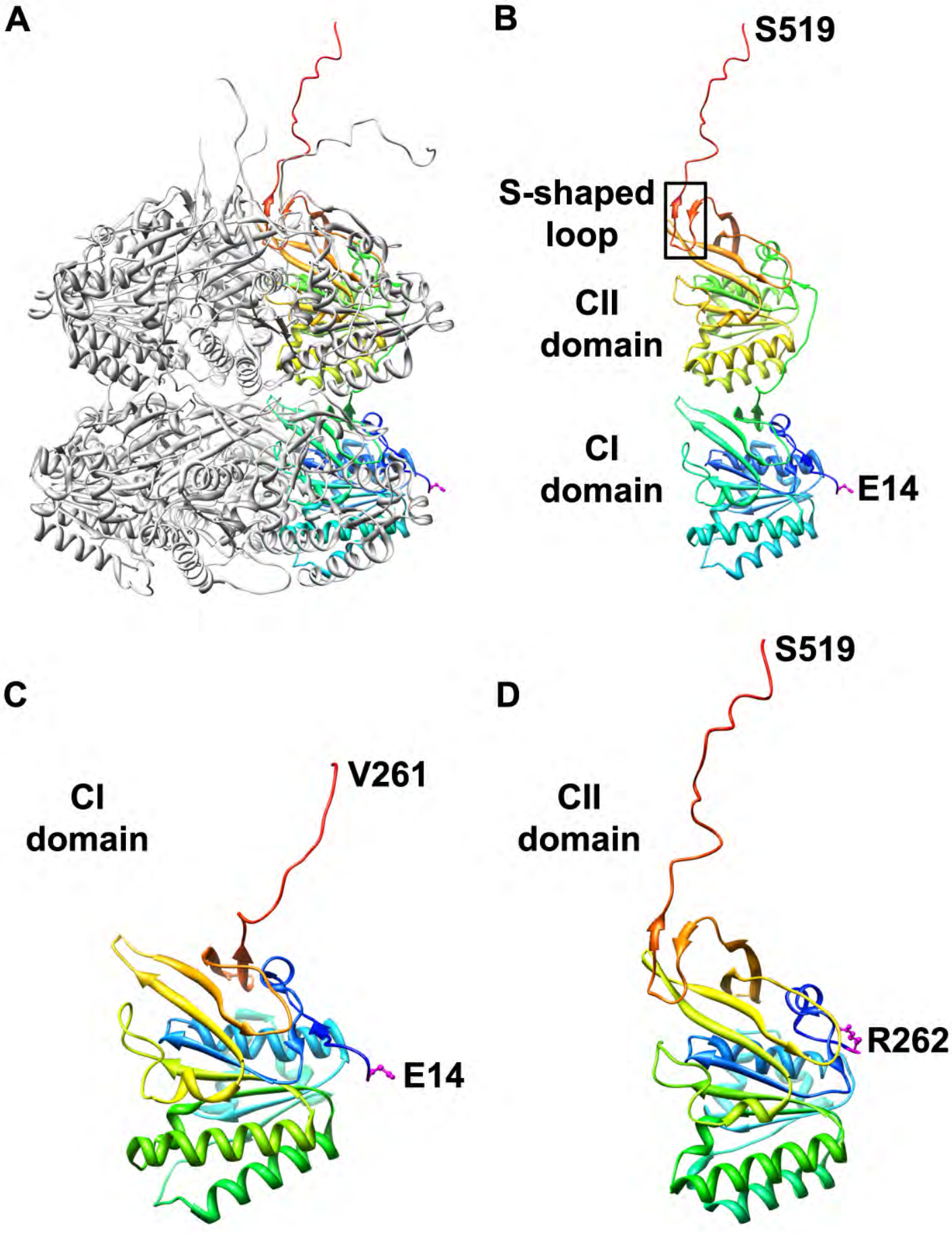
A
B
S519
S-shaped
loop
CII
domain
CI
domain
E14
C
V261
CI
domain
E14
D
S519
CII
domain
R262

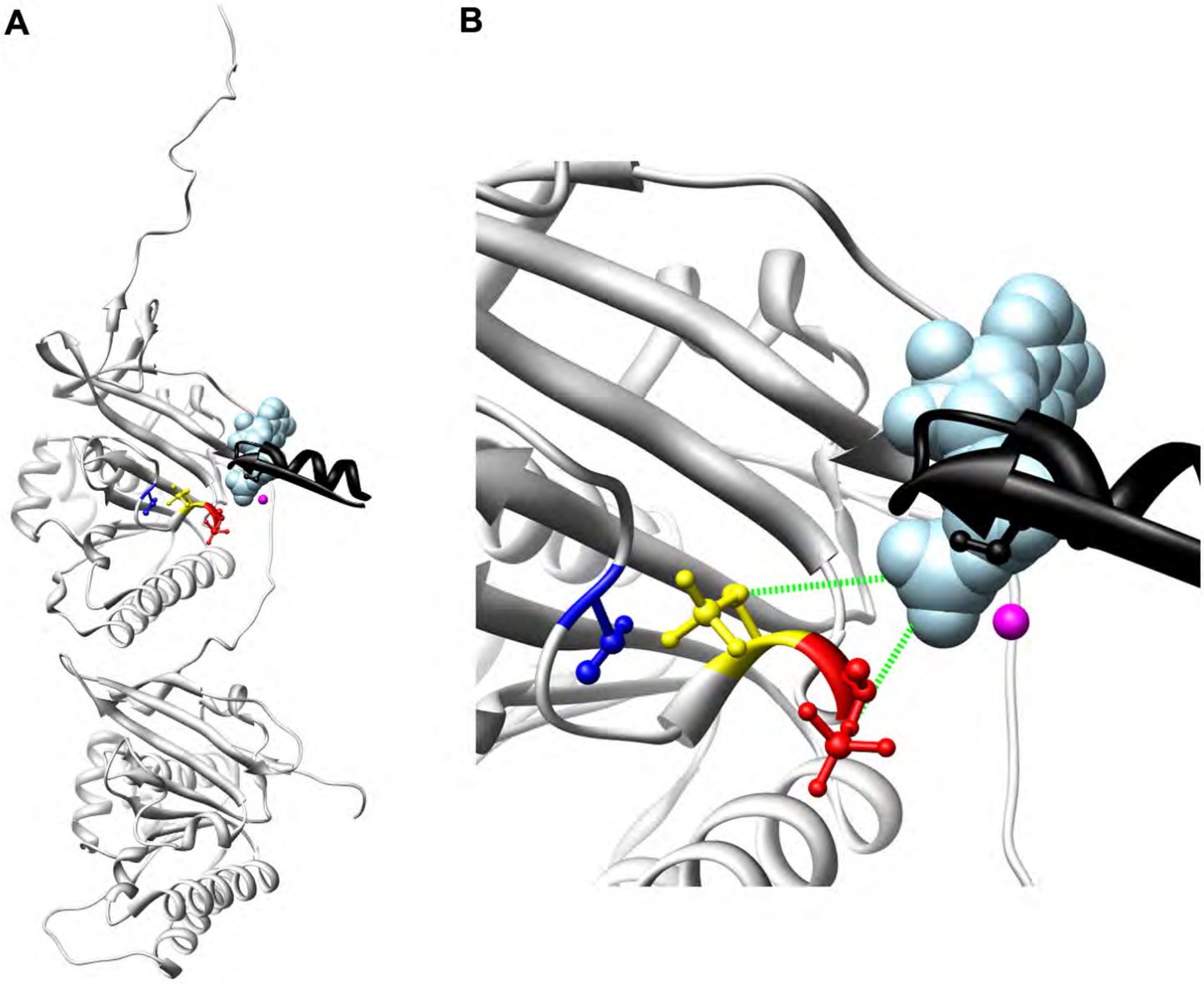
A
B

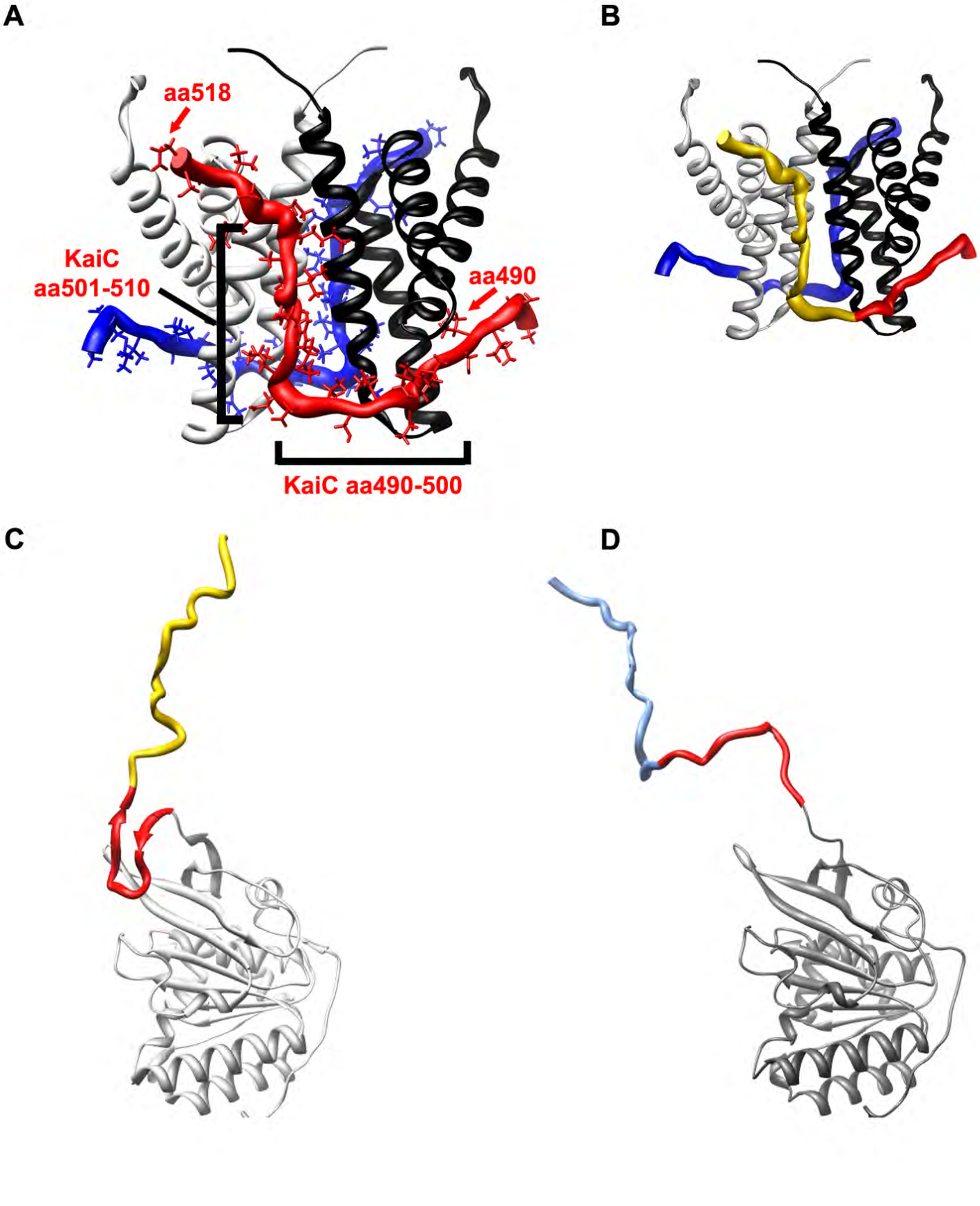
A
aa518
KaiC
aa501-510
aa490
KaiC aa490-500
B
C
D

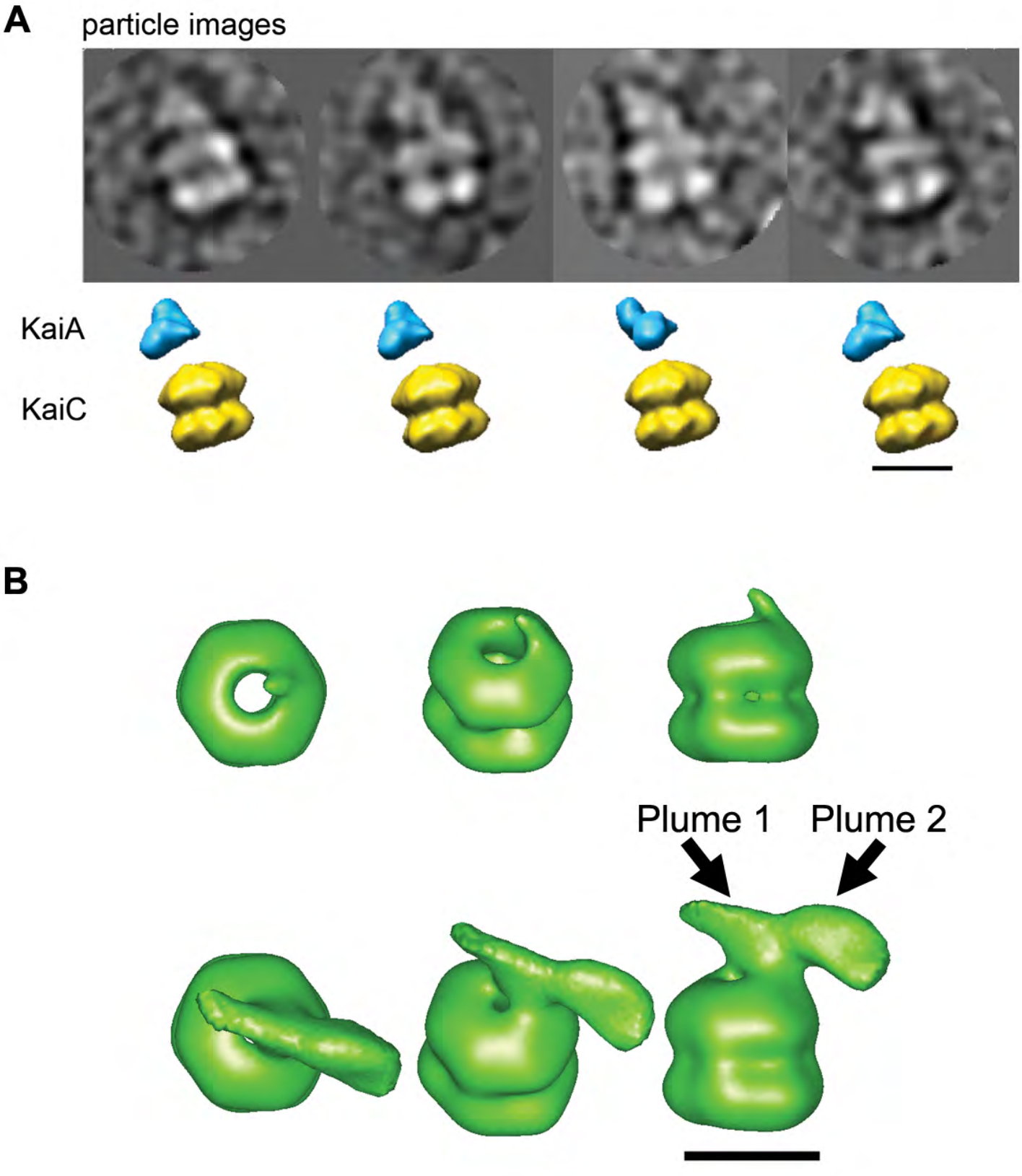
A
particle images
KaiA
KaiC
B
Plume 1
Plume 2

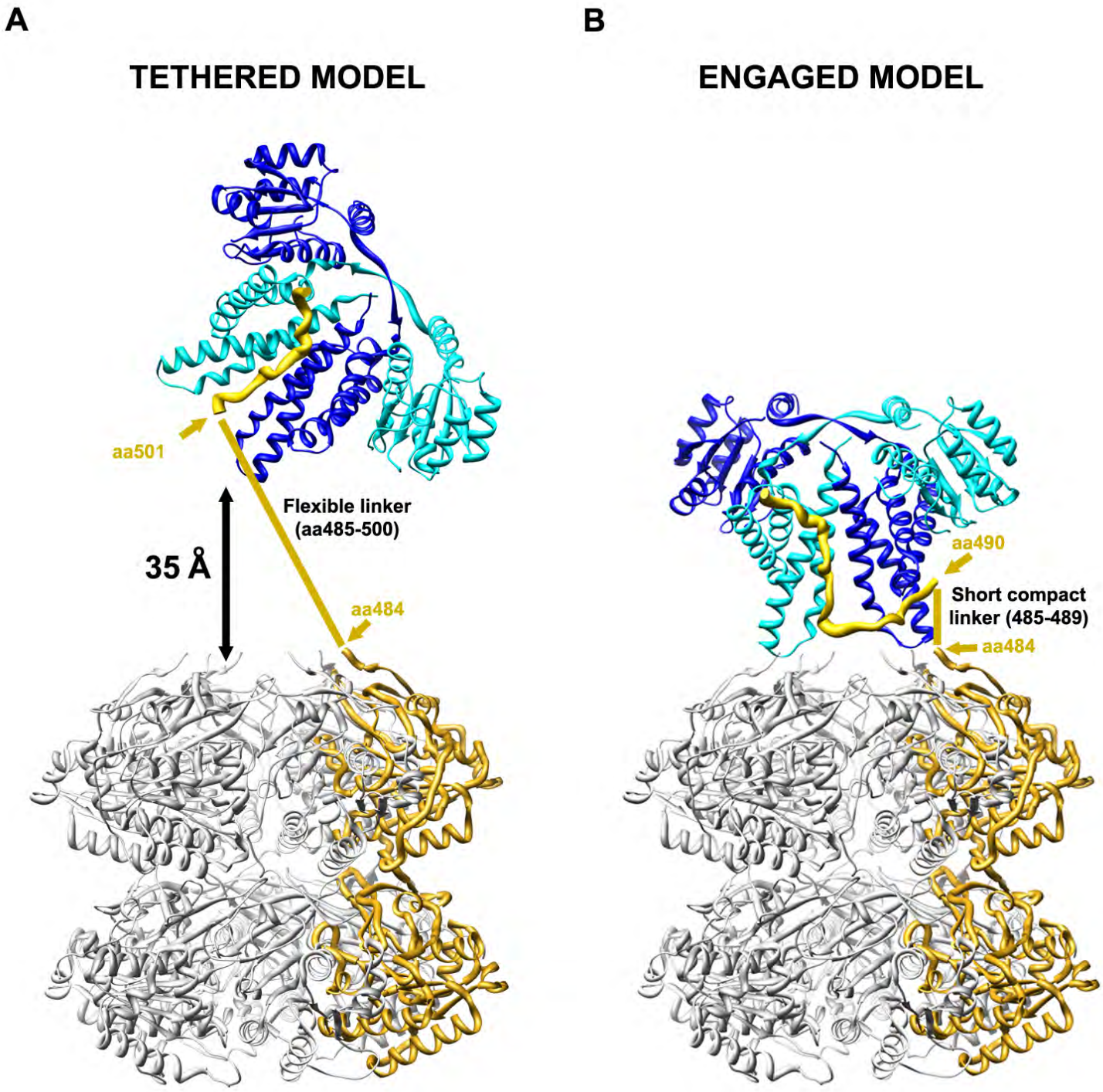
A
TETHERED MODEL
aa501
Flexible linker
(aa485-500)
35 Å
aa484
B
ENGAGED MODEL
aa490
Short compact
linker (485-489)
aa484